DE GRUYTER Journal of the Mechanical Behavior of Materials 2022; 31: 390–397

Research Article

Pham Van Dong, Nguyen Huu Phan*, Santosh Patil*, Shailesh Shirguppikar, Sudarshan Kalel, Le Thi Phuong Thanh, and Do Minh Hien

Effect of boron carbide reinforcement on properties of stainless-steel metal matrix composite for nuclear applications

https://doi.org/10.1515/jmbm-2022-0047
received January 19, 2022; accepted June 14, 2022

Abstract: Stainless steel (SS304) is a widely used material in underwater nuclear applications due to its superior corrosion resistance and high strength. Along with these superior properties, the application demands neutron absorption and high wear resistance under dynamic operations. The ceramic reinforcements help to enhance these properties of metal alloy with a suitable composite design. The present work deals with the development of high wear-resistant and radiation (nuclear) tolerant boron carbide (B_4C)–SS 304 composite material. SS304 metal matrix with 0–5 vol% of B_4C ceramic reinforcement is produced by powder metallurgy technique. The presence of reinforcement was confirmed with X-ray diffraction analysis. Properties such as density, hardness, and water absorption are measured. A pin-on-disc tribology study is conducted to evaluate the coefficient of friction and wear of developed compositions at a sliding distance of 200 m, contact load of 10 N, and sliding speed of 1 and 5 m/s under dry lubrication conditions. The lowest density of 2.96 g/cc was noted for 15% B_4C-reinforced composite as compared to the density of SS304 metal matrix (5.71 g/cc). The water absorption capacity of the composite was increased with percentage reinforcement, and it was found 62% higher than the unreinforced matrix. The hardness of composite increases with B_4C particle reinforcement and maximum microhardness of 153 HV was measured for 15 vol% reinforced composites. Wear and coefficient of friction decrease with an increase in the percentage of B_4C particles. At 15 vol% of B_4C in the composite, lowest wear (1.91 mm^3@1 m/s and 2.51 mm^3@5 m/s) and COF (0.021@1 m/s and 0.042@5 m/s) were observed. This suggests that the developed composite can be effectively used in low-pressure–high-speed nuclear applications.

Keywords: neutron absorption, stainless steel composite, B_4C, powder metallurgy, wear

1 Introduction

Mechanisms such as fueling machine, control rod drive, and shut down system in Pressurized Heavy Water Reactors at nuclear power facility utilize moving components like piston–cylinder arrangements, bush and roller bearings, ball screws, and gears. These mechanisms are categorized into two types: low pressure–high speed (*e.g.*, bearing, piston, and cylinder) and high pressure–low speed (*e.g.*, ball screws and gears) [1–3]. Since these mechanisms operate underwater, these components demand high corrosion resistance, along with nuclear radiation tolerance. Stainless steel (SS304) is one of the promising materials used for these applications because of its superior corrosion resistance, high strength, toughness, and good weldability [4,5]. However, this material suffers from insufficient wear resistance and radiation tolerance. The shortcomings of this metal alloy can be resolved by the incorporation of hard ceramic reinforcements. Ceramic reinforcements into the metal matrix improve the properties such as density, hardness, and wear resistance of the matrix material without

*** Corresponding author: Nguyen Huu Phan,** Department of Faculty of Mechanical Engineering, Hanoi University of Industry, No. 298, CauDien Street, Bac TuLiem District, Hanoi, Vietnam, e-mail: phanktcn@gmail.com
*** Corresponding author: Santosh Patil,** Department of Mechanical Engineering, RIT, Rajaramnagar affiliated to SU, Kolhapur, India, e-mail: santosh.patil@ritindia.edu
Pham Van Dong: Department of Science and Technology, Hanoi University of Industry, No. 298, CauDien Street, Bac TuLiem District, Hanoi, Vietnam
Shailesh Shirguppikar: Department of Mechanical Engineering, RIT, Rajaramnagar affiliated to SU, Kolhapur, India
Sudarshan Kalel: Institute of Nanoengineering and Microsystems, National Tsinghua University, Hsinchu, Taiwan
Le Thi Phuong Thanh, Do Minh Hien: Department of Faculty of Mechanical Engineering, Hanoi University of Industry, No. 298, CauDien Street, Bac TuLiem District, Hanoi, Vietnam

impacting corrosion resistance [6–9]. Among these ceramics, boron carbide (B_4C) is the third hardest material, with good chemical stability, high strength, and low density (2.52 g/cc). In addition, because of its ability to absorb neutrons, B_4C-reinforced composites can be effectively implemented for applications in nuclear industries [10,11]. Aluminum–B_4C composites have gained immense interest in the last decade for the production of wear-resistant and neutron absorbent materials, but these materials sometimes suffer from seizure and galling at high-pressure working conditions [2,12,13]. Recently, Sun *et al.* [14] developed B_4C-reinforced SS304 composite with neutron shielding properties wherein the B_4C content was optimized through the genetic algorithm program. With the incorporation of spherical carbide particles, the density was reduced by 33% and a significant increase in radiation tolerance was achieved. As mentioned earlier, the mechanism used for nuclear applications works under dynamic contact stress conditions, because of which, the SS–B_4C composites still demand to test tribological parameters such as wear and friction coefficient.

The properties of the composite depend upon the manufacturing method, reinforcing material, its fraction and distribution in the matrix, and interaction between the components [4,10,15,16]. Conventional methods like stir casting, powder metallurgy (PM), hot pressing, and extrusion along with some advanced methods like spark plasma sintering and physical vapor deposition are available for the fabrication of ceramic-reinforced metal matrix composite (MMC) [17–21]. With better material utilization, simplicity in the incorporation of hard materials into the matrix and proper distribution of particulates into the matrix, PM is a cost-effective technique to produce ceramic-reinforced metal composites [5,20–23]. On the other hand, porosity is induced in the composite structure during the sintering process which impacts the hardness of the material adversely [20,21]. Binder is a temporary means to mold the powder in the required shape by wetting the surface of particles and developing holding force between the particles. The binder material is usually incorporated during the blending process to wet the surface of powders for bonding and this binder is later evaporated during the sintering process. Stearic acid is an effective binder for iron matrix composite [24]; its insolubility in hot and cold water makes it suitable for underwater application.

Wear is a progressive loss of material when two materials are in contact with each other and there is a relative motion between them. The wear behavior of the material in nuclear applications decides the maintenance cycle and overall life of the material in extreme conditions. Wear depends upon the type of material, its microstructure, roughness, porosity, and hardness [2]. The hardness of any material affects the wear properties. The inclusion of a soft matrix with hard reinforcement increases the hardness along with the improvement of other properties such as density. An increase in the hardness of SS304–B_4C composite up to 7.5%, with reinforcement of 3% was reported by Balakrishnan and Rajesh [5]. Although the percentage of B_4C particles covered in ASTM A887 is only up to 0.25%, composites with ~16 and ~25% of B_4C reinforcement have been developed through PM and infiltration casting [14,23]. Comprehensive studies on fabrication and characterization of SS–B_4C MMC have been carried out [5,6,14,15,20–23] but none so far on the tribological behavior of SS–B_4C composite. Hence, the current study is focused on the development and tribological testing of B_4C–SS304 composite material for high-speed low contact pressure nuclear applications. Composites with 0, 5, 10, and 15% B_4C volume reinforcement by PM method are produced. The levels are selected to establish a general trend of the impact of B_4C particles on the tribology behavior of composites. To avoid the significant impact of porosity on the hardness of composite the reinforcement is limited to 15%. The tribology study of the developed composite is done by the pin-on-disk method under the dry sliding conditions to evaluate the coefficient of friction and wear properties. The effect of this B_4C reinforcement on density and water absorption is also evaluated. The next section is focused on details of materials and methods used for composite fabrication, methods for different material property testing followed by results and discussion.

2 Materials and methods

SS304 (or 18-8 steel) and B_4C in spherical powder form with an average particle size of 36 µm were used for the fabrication of cylindrical samples for the study. The typical contents of SS304 are presented in Table 1 [5,23]. PM involves the blending of powders, compaction into a particular shape under pressure with or without heat, followed by a sintering process.

B_4C powder with 0, 5, 10, and 15% of total volume was mixed with SS304 powder in planetary ball mill at 120 rpm with a 10:1 ball to powder ratio for 300 min. Ethanol of 2% was added as a processing agent. The mixed powders were dried and a 4% volume of stearic acid was added into the mixture as a binder. Then the mixture was uniaxially cold-pressed in a die at a pressure

Table 1: Composition of SS304 used

Element	vol%
Carbon	0.08
Chromium	18.21
Nickel	9.25
Manganese	2.00
Phosphorus	0.04
Silicon	1.00
Sulfur	0.03
Iron	Balance

of 400 MPa on a compression machine to obtain final cylindrical specimens with a size of 8 mm diameter and 30 mm length (Figure 1).

Sintering of cold-pressed specimen was conducted in vacuum furnace as follows: first the specimen was heated at the rate of 30°C/min up to 350°C and then kept for 5 min. Then, heated to the final temperature of 800°C and kept at this temperature for 10 min. Finally, the sample was cooled down in the furnace down to room temperature.

2.1 X-ray diffractometry (XRD)

XRD patterns of sample were recorded by Bruker X-ray diffractometer using (D2 Phaser model) Cu-Kα radiation with 1.5406 Å wavelength.

2.2 Density measurement

The specimen for the water absorption test was fabricated by the same procedure. Measurement of density and specific gravity was conducted according to ASTM D792 by using the simple Archimedes principle, *i.e.*, measuring the amount of water displacement. Three measurements were done for every three samples and the average was calculated. Specific gravity was obtained from using the following equation:

$$\text{Specific gravity} = \frac{a}{a-b},$$

where a is the apparent mass of specimen in air and b is the apparent mass of specimen completely immersed in water.

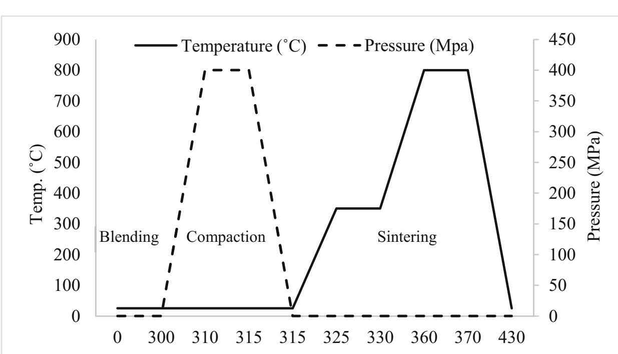

Figure 1: Time *vs* temperature *vs* pressure program followed for PM fabrication process which involves powder blending, cold compaction followed by vacuum sintering.

2.3 Water absorption capacity

A water absorption test was conducted to determine the amount of water absorbed under specified conditions which is important to check the performance of the material in the water exposed environment. The testing was conducted according to ASTM D570, where a disk specimen was prepared with a 2-in. diameter and 0.125-in. thickness by following a similar procedure. It is dipped in water at 23°C for 24 h. The specimen is weighed under wet and dry conditions and the percentage of water absorbed is given by the following formula:

$$\text{Percentage water absorption} = \frac{\text{Wet weight} - \text{Dry weight}}{\text{Dry weight}} \times 100.$$

2.4 Hardness measurement

Hardness and tensile strength of the material are often related; hardness also governs the amount of wear during the material contact. The Vickers microhardness tester was utilized to evaluate the hardness of the composites. By using a square pyramid indenter with 136°, a load of 1 kgf was applied for a period of 10 s. Each specimen was indented three times and the average was calculated. After the loading, the diagonals of indentation on the specimen are measured with the use of a microscope arrangement. By measuring the average length of diagonal, d, the Vickers hardness was calculated by using the formula:

$$\text{HV} = \frac{F}{A} \approx \frac{0.01819F}{d^2},$$

where F is in N and d is in mm.

2.5 Tribology test (wear and COF measurement)

The operating sliding speed <1 m/s, and contact pressure >1,000 MPa is considered for tribology testing of low-

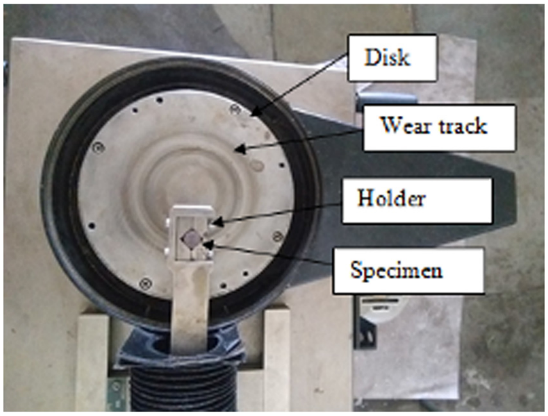

Figure 2: Pin-on-disc experimental arrangement for measurement of coefficient of friction and wear properties of specimen material. Here the disc is rotated while the specimen is stationary in the holder, the relative sliding motion between the disc and pin results in wear.

speed–high-pressure mechanisms in the nuclear industry [1,3]. As the study is focused on high-speed low contact pressure applications, sliding speed of 1 m/s and 5 m/s, and contact load of 10 N is considered for testing. Pin-on-disc setup was utilized to conduct the friction and wear tests at RIT, India (DUCOM, Bangalore, India, model: TR20-LE). Tests were conducted according to the ASTM G-99 standard. Before the test, the disc was cleaned thoroughly with solvent and clamped on a holder.

The cylindrical specimen (with 8 mm diameter and 30 mm length) was mounted in the holder above and in contact with the rotating disc as shown in Figure 2. The specimen was set above the wear disc using a height adjusting block. The test conditions are listed in Table 2, the sliding distance, track diameter, contact load, and ambient temperature were kept constant. Wear and frictional force were confirmed to zero before starting each test. During the test, the frictional force and wear were continuously recorded using a load cell and linear variable differential transformer sensor. The plots of wear, coefficient of friction (COF), and frictional force with time were displayed online during the test. Wear of the material in microns was noted down after each test. Three tests were conducted for each sample and an average was presented.

Table 2: Experimental conditions

Parameter	Operating conditions
Contact load	10 N
Track diameter	100 mm
Sliding velocity	1, 5 m/s
Sliding distance	200 m
Lubrication	Dry
Disc material	EN 31
Total disc diameter	200 mm
Roughness of disc material	1.6 μm Ra
Hardness of disc material	54 HRC
Environmental temperature	26°C
Relative humidity	60%

3 Results and discussion

Figure 3 shows the peaks in the XRD pattern of B_4C-reinforced composite. The peaks at 2θ values of 23.75, 35.54, and 37.60 correspond to B_4C on other hand peaks at 43.51, 75.40 correspond to Fe. At low reinforcement (5%) the peaks are hard to differentiate from the impurities; however, at high reinforcement (15%) these peaks are clearly seen. The increase in the intensity of peaks confirms the increase in the percentage of reinforcement.

The effect of percentage reinforcement on the density of the material is shown in Figure 4. The density of composite material depends upon the molecular interaction, porosity induced, and molecular configuration [3,7]. The composites with 0, 5, 10, and 15% B_4C reinforcement showed density of 5.71, 5.21, 4.20, and 2.96 g/cc, respectively. The incorporation of lighter reinforcement into the same volume of matrix results in a reduction of density with an increase in percentage reinforcement. Porosity is one of the undesirable properties associated with the PM technique which reduces the density of composite material. The porous structure is produced during the sintering process when the binder material is evaporated gradually, creating voids in the structure. However, this percentage of binder remained the same for all the compositions; hence, the porosity of material has negligible contribution to the density reduction of composite material as compared to the former reason.

As shown in Figure 4, the hardness of composite increases with the percentage of hard B_4C ceramic reinforcement. An increase in the hardness of composite is observed from 104 to 153 HV with 15% reinforcement of B_4C particles. The obvious increase in the hardness can be due to high strength B_4C reinforcement promoting good adhesion between steel matrix and B_4C, and uniform dispersion of reinforcement into the matrix [25]. However, during the cold compaction process, B_4C particles are displaced toward the sidewall, top, and bottom of the cylindrical sample under high compressive pressure. This higher presence of hard particles at the surface results in high surface hardness of composite materials [26]. Although the density and hardness of the given composite material are controlled by the light and hard B_4C particles, they are not directly related to each other.

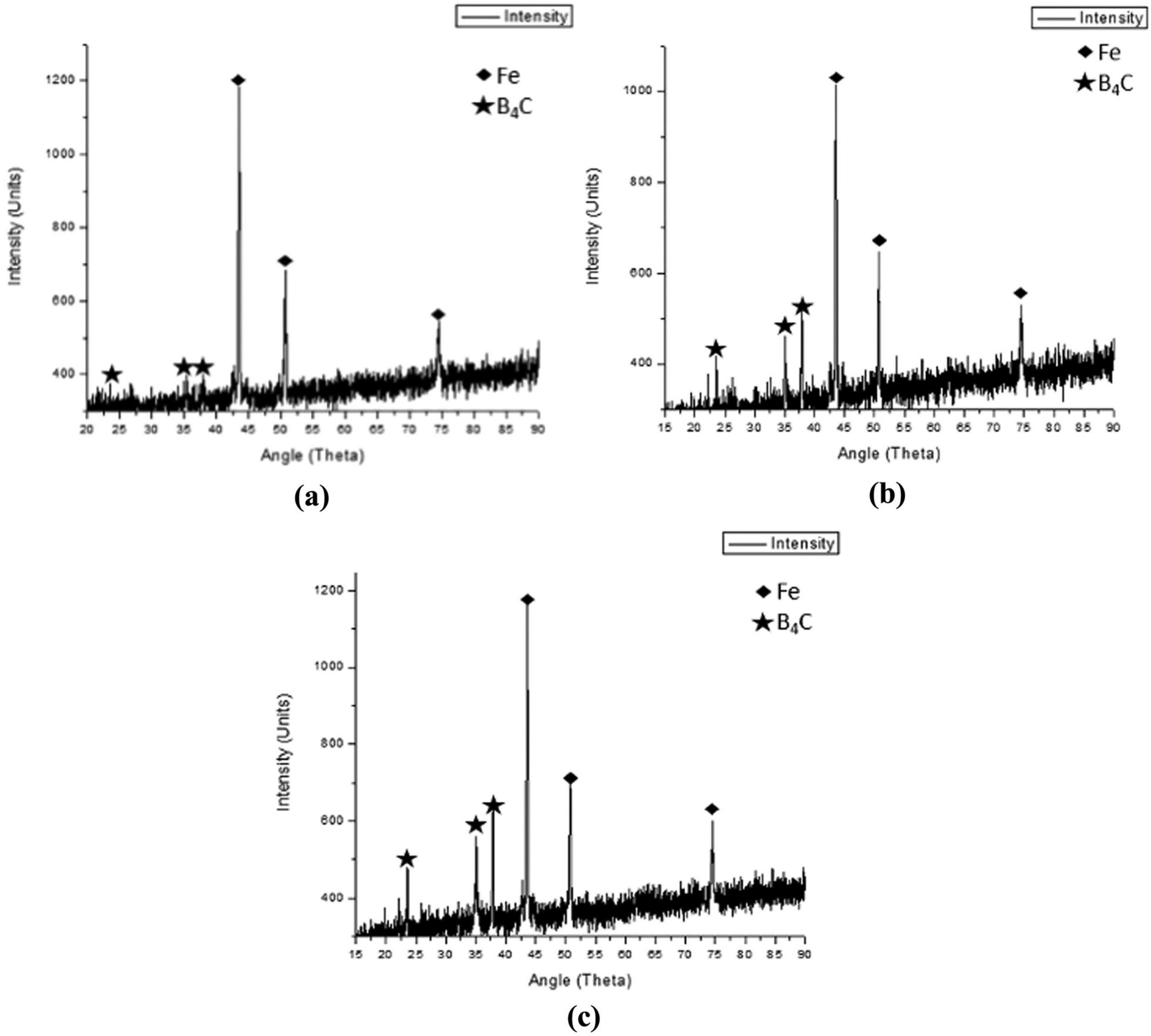

Figure 3: XRD patterns of sintered cold-pressed composite with B_4C reinforcement: (a) 5%, (b) 10%, and (c) 15%.

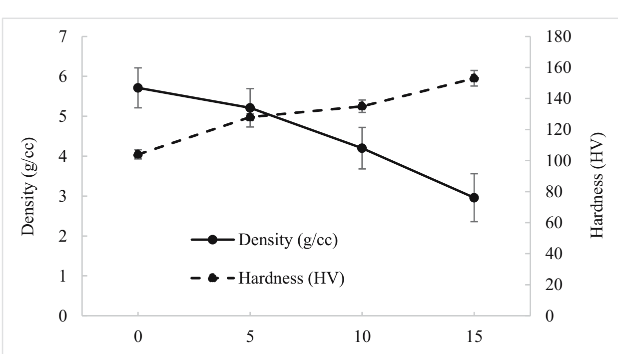

Figure 4: Effect of reinforcement on density and hardness of SS304–B_4C composite.

Water absorption is one of the important properties when the material is working underwater environment. The large presence of water or moisture in the material affects the useful properties such as strength and wear resistance during the working period of the material. It can be seen from the graph shown in Figure 5 that as the percentage of reinforcement increases, there is an increment in the absorption of water by the composite material. The percentage of water absorbed by the material with 0, 5, 10, and 15% of reinforcement is 0.27, 0.34, 0.53, and 0.71, respectively. Due to induced porosity, the voids in the material are filled by water resulting in more water absorption. This property can affect the wear behavior of the composite when the material is under

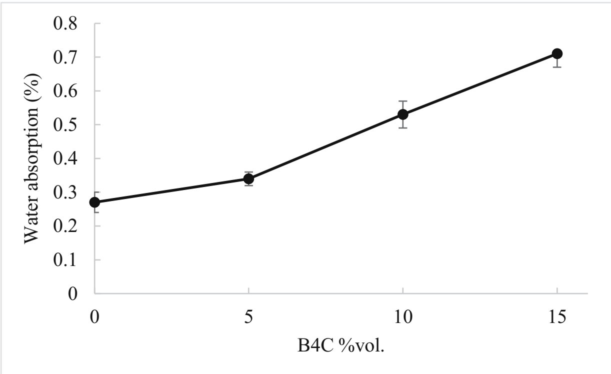

Figure 5: Effect of reinforcement on the water absorption capacity of SS304–B_4C composite material.

sliding motion. The type of materials used in composites, additives, and binders, and temperature and length of exposure are the factors affecting the water absorption property of the composite material.

To investigate the effect of B_4C particles on the wear of the composite, parameters such as sliding velocity and sliding distance are kept constant. From Figure 6 wear amount and coefficient of friction gradually reduce with an increase in B_4C percentage. At 15% B_4C, composite exhibits lowest wear (1.91 mm^3@1 m/s and 2.51 mm^3@5 m/s) and COF (0.021@1 m/s and 0.042@5 m/s), respectively. Whereas

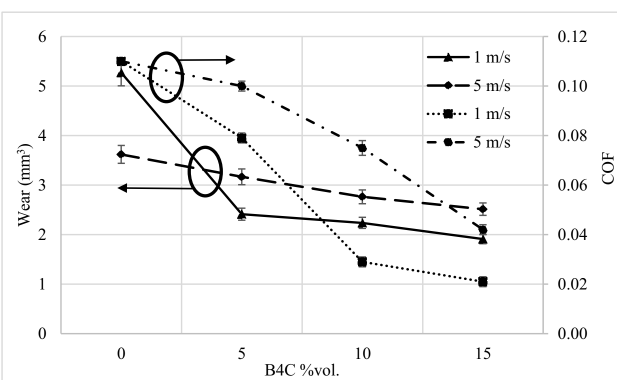

Figure 6: The effect of B_4C vol% reinforcement on wear and COF of composite material.

the pure SS304 sample exhibits the largest value of wear (5.67 mm^3@1 m/s and 3.62 mm^3@5 m/s) and COF (0.110@1 m/s and @5 m/s), respectively. The decrease in the wear and COF is contributed by the hardness of the composite, according to the well-known Archard equation [25]. As the contacting surfaces are iron alloys, and tests are performed under the presence of air, the oxygen from air forms an oxide layer on the surface of iron alloy. A mechanically mixed layer (MML) is developed that has a low coefficient of friction and this layer reduces the direct contact between pin and disc material and avoids the occurrence of adhesive mechanism [2,3,27]. Milling of powders during fabrication leads to stability of this tribological layer and improvement in the wear resistance property of the material [7,25]. The worn surfaces of highly reinforced composite pins after the test are covered with grooves which denote abrasive wear. Whereas the pure SS304 pins show plastic deformation and dominance of adhesive wear for softer composite structures. Thus, the hard particles in the structure transform the wear mechanism from adhesive to abrasive type. The B_4C particles actively participate in the load-bearing mechanism during contact and have a low tendency to adhere to the counter surface, reducing the possibility of stick–slip phenomena. From the discussion, the composite material with 15% of B_4C reinforcement exhibits better properties compared to other compositions. The comparison of wear volume for different composites found in literature is shown in Table 3.

The pure ceramic and ceramic composite coating approach have proved itself for improving wear resistant and friction coefficient properties of metals. The friction coefficient of the B_4C/a-C coatings under sliding condition is reported as 0.2 for less than 1,000 cycles [28]. Whereas the SS304–B_4C composite shows maximum friction coefficient of 0.11 for less than 1,000 cycles. Although the ceramic coating wear resistant approach appears promising in the B_4C-based coating, boric acid is formed at the sliding interface in the presence of water vapors. Since many of the applications in nuclear industry work underwater environment, coating-based approach could cause severe problems. On the other hand, the uniform distribution of B_4C particles

Table 3: Comparison of wear volume for different composites

B_4C and SS composites	Contact load (N)	Sliding distance (m)	Sliding speed (m/s)	Wear volume (mm^3)	Reference
AA5083/5% B_4C	30	1,000	1	5	[29]
SS304/20% TiB_2	15	500	1	3	[30]
AA-5%SiC–5% B_4C	20	3,000	3	2.21	[31]
SS304/15% B_4C	10	200	1	1.91	This study

in metal matrix does not promote this behavior and at the sliding interface is dominated by MML rather.

4 Conclusion

The work presents the effect of the percentage of B_4C reinforcement on the properties of SS304 mainly density, water absorption capacity, hardness, COF, and wear of composite material. The density of 15% B_4C-reinforced composite was found lowest (2.96 g/cc) compared to the density of SS304 metal matrix (5.71 g/cc). There was a ~48% reduction in the density due to increasing lighter reinforcement into the same volume of the metal matrix. The water absorption capacity of the composite was increased with percentage reinforcement, and it was found 62% higher than pure SS304 due to the accumulation of moisture or water content at the available spaces within the material, generated because of porosity. A maximum microhardness of 153 HV was noted for 15% reinforced composite. Wear and COF of the composite are inversely proportional to the percentage reinforcement because of increased hardness. The proper distribution of B_4C particles through PM and the presence of an oxide layer at the contact during operation stabilizes the wear process due to which wear and COF at 15% of reinforcement is the lowest than the pure material at different sliding velocities.

Funding information: The authors state no funding involved.

Author contributions: All authors have accepted responsibility for the entire content of this manuscript and approved its submission.

Conflict of interest: The authors state no conflict of interest.

References

[1] Khare N, Limaye PK, Singh K, Jadhav DT, Bute A, Kalel N. Experimental and theoretical analysis of zircaloy-4 and AISI 304 stainless steel material pair in water sliding conditions. Adv Tribol. 2018;2018:1–7.
[2] Shinde DM, Sahoo P, Davim JP. Tribological characterization of particulate-reinforced aluminum metal matrix nanocomposites: a review. Adv Compos Lett. 2020;29:1–28.
[3] Bute A, Khare N, Kumar S, Bhattacharya D, Singh K, Sahu AK, et al. Tribological properties of hydrogenated boron carbide (BxC:Hy) thin films on stainless steel deposited by RF-PECVD technique. Eur Phys J Appl Phys. 2020;91(2):1–12.
[4] Baldev R, Kamachi Mudali U, Vijayalakshmi M, Mathew MD, Bhaduri AK, Chellapandi P, et al. Development of stainless steels in nuclear industry: with emphasis on sodium cooled fast spectrum reactors history, technology and foresight. Adv Mater Res. 2013;794:3–25.
[5] Balakrishnan N, Rajesh R. Fabrication and analysis of 304 stainless steel boron carbide metal matrix composite. Int J Mech Eng Technol. 2018;9:33–42.
[6] Pagounis E, Lindroos VK. Processing and properties of particulate reinforced steel matrix composites. Mater Sci Eng A. 1998;246(1):221–34.
[7] Varol T, Çanakç1 A. Effect of weight percentage and particle size of B_4C reinforcement on physical and mechanical properties of powder metallurgy Al2024–B_4C composites. Met Mater Int. 2013;19:1227–34.
[8] Saxena A, Singh N, Kumar D, Gupta P. Effect of ceramic reinforcement on the properties of metal matrix nanocomposites. Mater Today Proc. 2017;4(4, Part E):5561–70.
[9] Martín F, García C, Blanco Y, Rodriguez-Mendez ML. Influence of sinter-cooling rate on the mechanical properties of powder metallurgy austenitic, ferritic, and duplex stainless steels sintered in vacuum. Mater Sci Eng A. 2015;642:360–5
[10] Matović B, Maletaškić J, Prikhna T, Urbanovich V, Girman V, Lisnichuk M, et al. Characterization of B_4C–SiC ceramic composites prepared by ultra-high pressure sintering. J Eur Ceram Soc. 2021;41(9):4755–60.
[11] Chen XG. Application of AL–B_4C metal matrix composites in the nuclear industry for neutron absorber materials. TMS Annu Meet. 2006;2006:343–50.
[12] Prasad NE, Wanhill RJ. Aerospace materials and material technologies. Singapore: Springer; 2017.
[13] Shikalov VS, Vidyuk TM, Kosarev VF, Klinkov SV. Effect of B_4C content on microhardness and sliding wear behavior of cold sprayed aluminum matrix coatings. AIP Conf Proc. 2021;2351(1):040060.
[14] Sun W-Q, Hu G, Yu XH, Shi J, Xu H, Wu RJ, et al. Study on a high-boron-content stainless steel composite for nuclear radiation. Materials. 2021;14(22):7004.
[15] Akhtar F. Ceramic reinforced high modulus steel composites: processing, microstructure and properties. Can Metall Q. 2014;53(3):253–63.
[16] Guo H, Zhang Z. Processing and strengthening mechanisms of boron-carbide-reinforced aluminum matrix composites. Met Powder Rep. 2018;73(2):62–7.
[17] Sahu PS, Banchhor R. Fabrication methods used to prepare Al metal matrix composites-A. Int Res J Eng Technol. 2016;3(10):123–32.
[18] Malaki M, Xu W, Kasar AK, Menezes PL, Dieringa H, Varma RS, et al. Advanced metal matrix nanocomposites. Metals. 2019;9(3):330.
[19] Moreira AB, Ribeiro L, Lacerda P, Pinto A, Vieira MF. Production and characterization of austenitic stainless steel cast parts reinforced with wc particles fabricated by ex situ technique. Materials. 2021;14(24):7855.

[20] Chuankrerkkul N, Lorchaiyanunt C, Tansittipan S, Polsilapa S. Powder metallurgy of stainless steel–tungsten carbide composites. ICCM International Conferences on Composite Materials; 2009 Jul 27–31; Edinburgh, UK. IOM Communications; 2009.
[21] Oke SR, Ige OO, Falodun OE, Okoro AM, Mphahlele MR, Olubambi PA. Powder metallurgy of stainless steels and composites: a review of mechanical alloying and spark plasma sintering. Int J Adv Manuf Technol. 2019;102:3271–90.
[22] Sharifi EM, Karimzadeh F, Enayati MH. Fabrication and evaluation of mechanical and tribological properties of boron carbide reinforced aluminum matrix nanocomposites. Mater Des. 2011;32:3263–71.
[23] Elayidom MR, Abhishek AS, Mohan A, Vijayakumar A, Rajesh R, Balakrishnan N, et al. Fabrication of stainless steel matrix composites containing up to 15%boron carbide. Int J Adv Chem Sci Appl. 2017;5(1):21–4.
[24] Shamsuddin S, Jamaludin SB, Hussain Z, Ahmad ZA. Influence of binder in iron matrix composites. AIP Conf Proc. 2010;1217(1):419–23.
[25] Alizadeh A, Maleki M, Abdollahi A. Preparation of super-high strength nanostructured B_4C reinforced Al-2Cu aluminum alloy matrix composites by mechanical milling and hot press method: microstructural, mechanical and tribological characterization. Adv Powder Technol. 2017;28(12):3274–87.
[26] Saadatmand M, Aghazadeh Mohandesi J. Optimization of mechanical and wear properties of functionally graded Al6061/SiC nanocomposites produced by friction stir processing (FSP). Acta Metall Sin. 2015;28(5):584–90.
[27] Fernandes CM, Vilhena LM, Pinho CMS, Oliveira FJ, Soares E, Sacramento J, et al. Mechanical characterization of WC–10wt% AISI 304 cemented carbides. Mater Sci Eng: A. 2014;618:629–36.
[28] He D, Shang L, Lu Z, Zhang G, Wang L, Xue Q. Tailoring the mechanical and tribological properties of B_4C/a-C coatings by controlling the boron carbide content. Surf Coat Technol. 2017;329:11–8.
[29] Singh R, Shadab M, Dash A, Rai RN. Characterization of dry sliding wear mechanisms of AA5083/B_4C metal matrix composite. J Braz Soc Mech Sci Eng. 2019;41(98):1–11.
[30] Tjong SC, Lau KC. Sliding wear of stainless steel matrix composite reinforced with TiB_2 particles. Mater Lett. 1999;41(4):153–8.
[31] Thirumalai Kumaran S, Uthayakumar M, Aravindan S. Analysis of dry sliding friction and wear behaviour of AA6351–SiC–B_4C composites using grey relational analysis. Tribol – Mater Surf Interfaces. 2014;8(4):187–93.